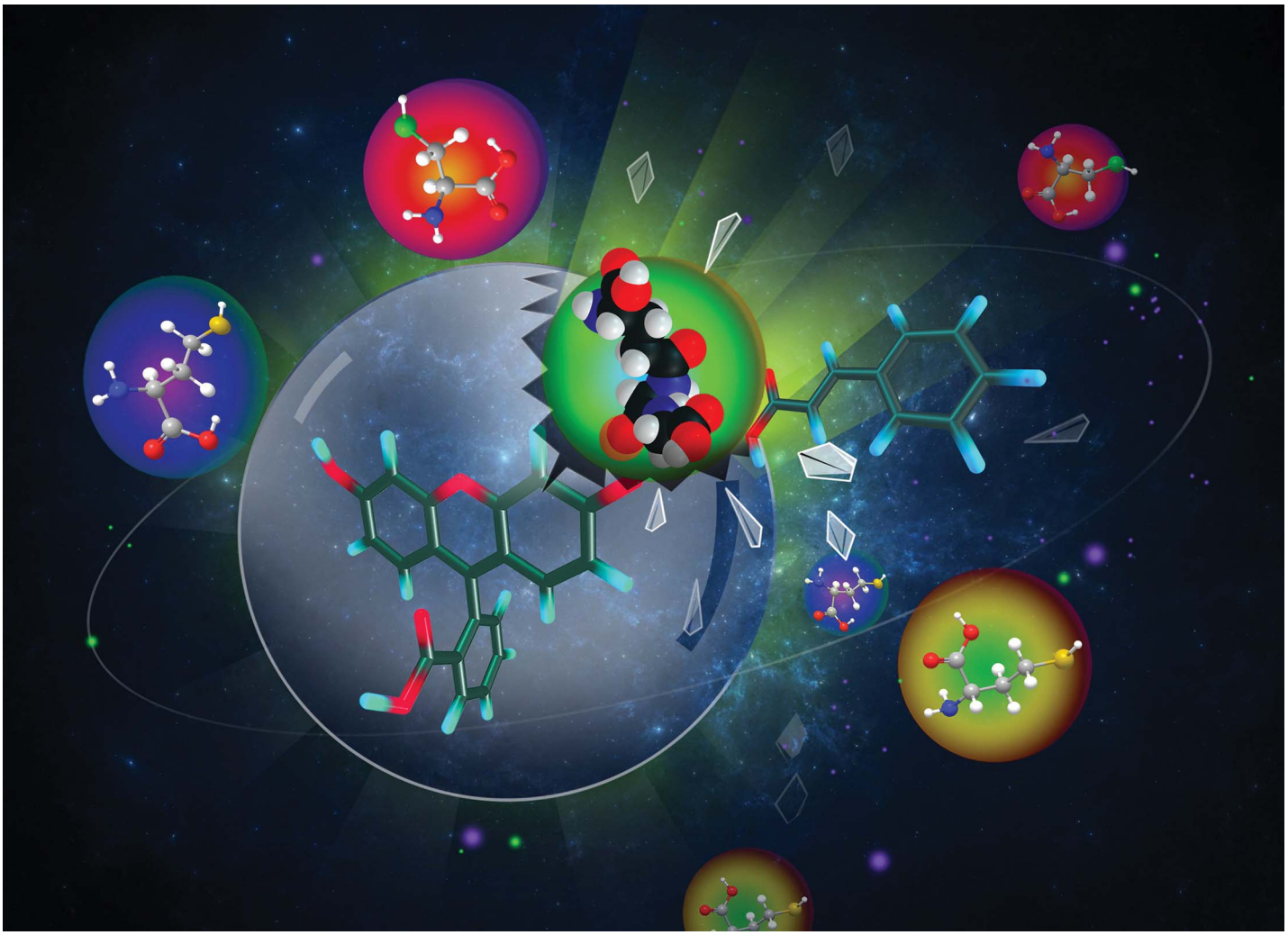

**Showcasing research from Professor Jianli Li's laboratory, Ministry of Education Key Laboratory of Synthetic and Natural Functional Molecule Chemistry, College of Chemistry & Materials Science, Northwest University, Xi'an, China, and Professor Fulin Chen's laboratory, Ministry of Education Key Laboratory of Resource Biology and Modern Biotechnology in Western China, The College of Life Sciences, Northwest University, Xi'an, China.**

Fluorescent probes guided by a new practical performance regulation strategy to monitor glutathione in living systems

A practical regulation strategy to improve the recognition performance of GSH specific probe have been constructed by the guidance of theoretical simulation. The conjugative effect-enhanced acrylate moiety could provide a remarkable selectivity for GSH over other thiols. Electron donor groups can increase this effect, but substituent groups on the olefinic bond and electron withdrawing groups show the opposite effect. This strategy has profound significance for improving the recognition performance of reaction-based probes.

## As featured in:

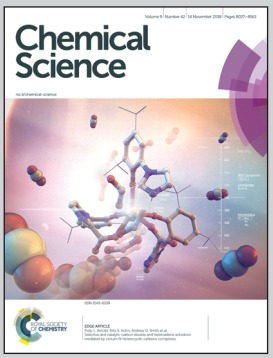


See Fulin Chen, Jianli Li *et al.*, *Chem. Sci.*, 2018, **9**, 8065.

ROYAL SOCIETY OF CHEMISTRY

rsc.li/chemical-science

Registered charity number: 207890

Chemical Science

EDGE ARTICLE

View Article Online
View Journal | View Issue



Cite this: *Chem. Sci.*, 2018, **9**, 8065

All publication charges for this article have been paid for by the Royal Society of Chemistry

Received 1st August 2018
Accepted 19th September 2018

DOI: 10.1039/c8sc03421d

rsc.li/chemical-science



# Fluorescent probes guided by a new practical performance regulation strategy to monitor glutathione in living systems†

Mengyao She, ‡[ab] Zhaohui Wang, ‡[a] Tianyou Luo,[a] Bing Yin,[a] Ping Liu,[a] Jing Liu,[b] Fulin Chen,*[b] Shengyong Zhang[a] and Jianli Li *[a]

Glutathione (GSH) plays an important role in the body's biochemical defense system, and the detection of GSH in a physiological system is an important tool for understanding redox homeostasis. Protection–deprotection strategies have proven to be the most reliable, among existing detection methods. However, the understanding of how various electronic and steric effects influence a probe's ability to recognize a substrate is still lacking. In this study, we have analyzed various substituent effects on a GSH probe template *via* theoretical calculations and constructed the performance regulation and control strategy for this kind of probe. We then developed a series of guided probes using eighteen different acrylic ester derivatives to mask the fluorescence of fluorescein. The optical performance differences between the guided probes strongly supported the applicability of our proposed guiding strategy. Moreover, the positively guided probes are excellent for imaging GSH distribution in living cells and mice.

## Introduction

Biological thiols, such as cysteine (Cys), homocysteine (Hcy), and glutathione (GSH), exert crucial physiological functions in health and disease states.[1–3] Thiols play important roles in cellular biochemical defense, especially in redox homeostasis, which maintains the equilibrium of reduced free thiols and oxidized disulfides.[4–7] As such, the development of practical tools to quantify thiol fluctuation in biological systems has significant values.[8,9]

Strategies for detecting biological thiols have undergone rapid development during the past few years and will continue for the foreseeable future.[10–14] Protection–deprotection of signal groups has proven to be an effective and reliable method to detect biological thiols, among numerous detection mechanisms.[15] Countless fluorescent probes for biological thiol detection based on this strategy have appeared during the past decade.[16–19] However, due to the similar chemical characteristics of each probe, they cannot distinguish one specific thiol from another in the complicated physiological environment of the cells. Thus, there is a critical need for improved probes that bind to specific thiols.

It is well known that GSH is at a higher concentration than Cys or Hcy in living organisms during physiological processes, especially in cell growth, metabolism, oxidative stress, and even cancer therapy.[20–23] Construction of fluorescent probes to detect GSH has drawn a lot of attention in the past few years, and it is acknowledged that acrylic esters could act as powerful modular moieties for GSH *via* Michael addition reactions.[24,25] However, there are still no universal strategies to regulate the performance of this type of probe during its design, synthesis, and application, and the detailed mechanisms of action influenced by substituent groups are still poorly understood.[26–29]

Based on the typical mechanism of a protection–deprotection probe, we can reasonably infer that introducing an electron donor/acceptor or sterically hindered groups on an α,β-unsaturated ketone substituted moiety could regulate the effect of GSH detection. And choosing suitable substituent groups may increase the selectivity and sensitivity of the probe.

To verify this conjecture and achieve the objective of constructing a GSH-specific probe, we established a theoretical template for a protection–deprotection probe, using fluorescein as the signal scaffold, and by decoration with different acrylic ester derivatives (Fig. 1). The structural characteristics of these elaborately designed probes have been analyzed *via* DFT calculations, and their reaction activities with GSH were predicted by energy calculation, frontier orbital theory, and the Fukui function, which have direct significance to the design of a GSH-specific probe.

[a]*Ministry of Education Key Laboratory of Synthetic and Natural Functional Molecule Chemistry, College of Chemistry & Materials Science, Northwest University, Xi'an, Shaanxi 710127, PR China. E-mail: lijianli@nwu.edu.cn*

[b]*Key Laboratory of Resource Biology and Modern Biotechnology in Western China, Ministry of Education, Northwest University, 229 TaiBai North Road, Xi'an, Shaanxi Province, 710069, PR China. E-mail: chenfl@nwu.edu.cn*

† Electronic supplementary information (ESI) available: Details of synthesis, characterization data and theoretical calculation of all probes; computational details. See DOI: 10.1039/c8sc03421d

‡ These authors contributed equally to this work.

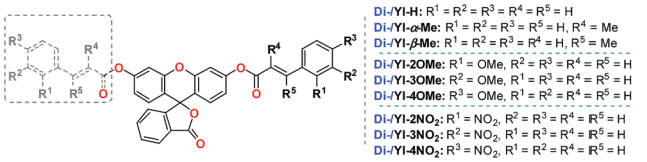


Fig. 1 The general template for GSH probes based on protection–deprotection of fluorescein by acrylic ester derivatives.

Based on the simulation results we proposed a practical regulation and control strategy for GSH-specific probes and synthesized the relevant probes that were contained in the probe template. The optical detection performance of our GSH probes strongly demonstrates the viability of this design strategy. Moreover, the positively guided probes revealed excellent applicability for imaging GSH distribution in living cells and mice.

## Results and discussion

### Establishment and analysis of the theoretical template

According to previous reports,[30,31] an acrylate moiety leaves easily through a Michael addition reaction, under the triggering effect of thiols, and then releases the fluorogen, emitting fluorescence. Although this mechanism has been provided by numerous research studies in the past few years, there is still a lack of necessary research about the details of electronic and steric effects during this process.[32,33] In this work, we chose methoxyl as the electron donor group and nitryl as the electron withdrawing group and introduced methyl to provide appropriate steric hindrance. We established a general molecular template using Density Functional Theory *via* the Gaussian 09 program.[36,37]

To further clarify these substituent effects from a theoretical perspective, a series of electrostatic charges and bond energies were calculated and are shown in Table 1. As shown by the preliminary estimation, the electron-donating group could apparently enhance the electron cloud density around the enone β carbon, lower the reactivity, and promote the selectivity to the strong nucleophile GSH. These effects are completely converse when the electron-withdrawing group takes effect.

Table 1 Calculated electrostatic charges of the enone β carbons (eV), bond dissociation energies (BDES, kJ mol$^{-1}$) of the ester bonds and formation enthalpies (kJ mol$^{-1}$) of the C–S bonds in the GSH probe recognition intermediate

| Probe | Electrostatic charges | BDES | Formation enthalpy |
|---|---|---|---|
| **Fl-H** | −0.122 | 273.38 | −192.15 |
| **Fl-αMe** | −0.14 | 267.96 | — |
| **Fl-βMe** | 0.097 | 268.01 | — |
| **Fl-2OMe** | −0.136 | 275.00 | −186.45 |
| **Fl-3OMe** | −0.132 | 274.77 | −182.93 |
| **Fl-4OMe** | −0.14 | 273.87 | −179.91 |
| **Fl-2NO$_2$** | −0.13 | 265.34 | — |
| **Fl-3NO$_2$** | −0.122 | 212.64 | — |
| **Fl-4NO$_2$** | −0.118 | 225.74 | — |

Furthermore, the bond dissociation energies (BDES) of ester bonds dwindled significantly when the strong electron-donating group, methoxyl, was introduced into the molecular skeleton. In contrast, the electron-withdrawing group exhibited the opposite effect, which manifested the inert reactivity of probes **Fl-2/3/4OMe**. Methyl substituents at *α*/*β* sites caused slight BDES reductions, suggesting the instability of **Fl-*α*/*β*OMe** to alkalescence. In addition, the formation enthalpy of a C–S bond in the recognition intermediate **probe-GSH** unequivocally demonstrated that the electron-donating group is capable of further passivating esterolytic action after being stabilized by a benzene ring, and endowing the probe with a unique selectivity for GSH.

The HOMO–LUMO energies, gaps and spatial distributions for each probe were determined and are displayed in Fig. 2. All the LUMOs of these probes were located on the recognition part, where the typical nucleophilic addition reaction would proceed. The HOMOs of probes **Fl-*α*/*β*Me** and **Fl-2/3/4NO$_2$** were distributed on the xanthene moieties, and were separated from the distributions of their LUMOs. However, for probes **Fl-2/3/4OMe**, both LUMOs and HOMOs are distributed in the recognition part of the probe. More notably, as electron acceptors, the LUMO energies of **Fl-2/3/4NO$_2$** are much lower than those of other probes, which means that these probes are more susceptible to attack by the HOMOs of GSH, –OH or –HS (calculated energies, −6.8329 eV, −5.4993 eV, −5.4448 eV, respectively). These structural characteristics might be the reason for their instability.

The Fukui$^+$ function[34,35] was also employed to evaluate the likelihood of a nucleophilic attack by GSH/thiols/–OH on each probe (Fig. 3). Collectively, the Fukui$^+$ functions are nearly all concentrated on alkene bonds and carbonyl C atoms, and the Fukui$^+$ function values of the *β*-sites are much larger than those of other active sites, indicating that the *β*-site is the first choice for nucleophilic attack by GSH/thiols/–OH.

Fluorescein protected by cinnamic acid (**Fl-H**) was stabilized by conjugated groups (benzene) and passivated the reaction activity of the *β*-site of the carbonyl group to ensure that the

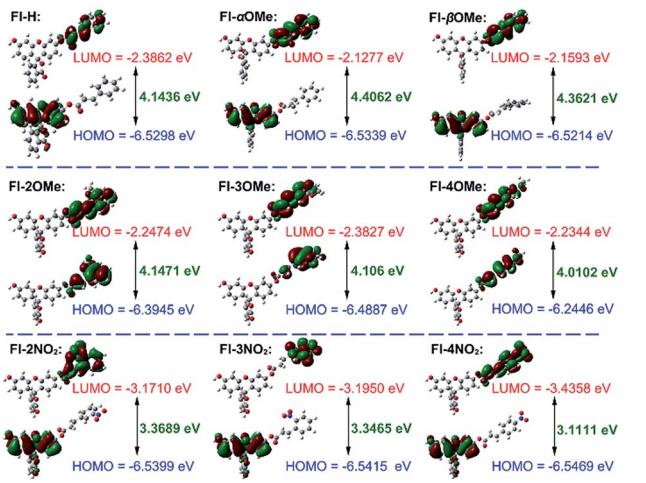


Fig. 2 HOMO–LUMO energy values and gaps and their distributions in all probes.

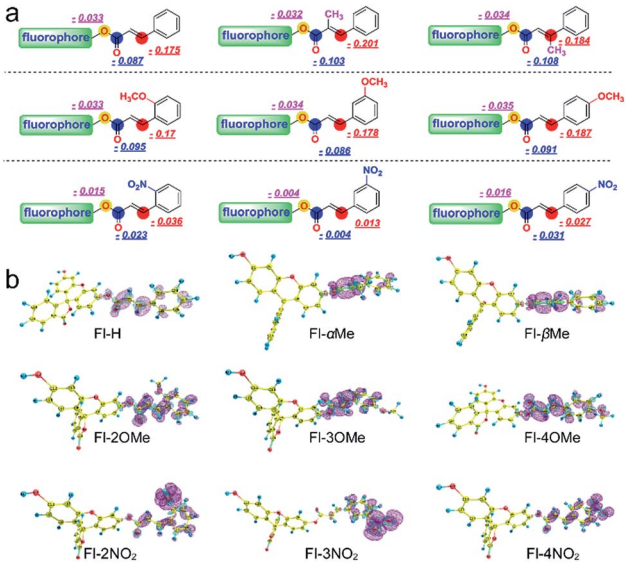


Fig. 3 (a) Fukui$^+$ function value of the core site; (b) Fukui$^+$ functional distributions.

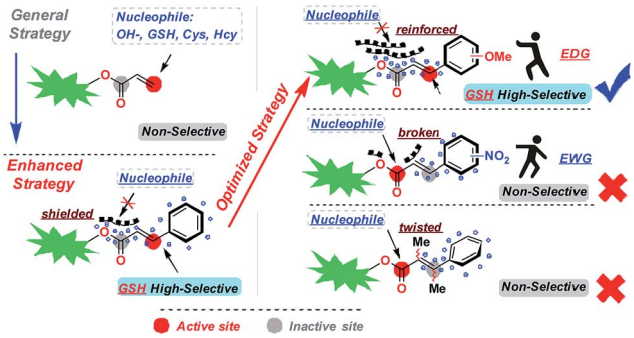


Fig. 4 General and proposed performance control strategy for the design of GSH-specific probes.

Michael addition reaction could only be triggered by GSH with its high p$K_a$ and nucleophilic attack ability. The introduction of a methyl group into the $\alpha/\beta$ site of the carbonyl will cause structural torsion and cause the maintenance of coplanarity between the alkene and benzene (dihedral angle: **Fl-H** = 0.08°; **Fl-αMe** = 30.42°; **Fl-βMe** = 33.72°, Fig. S31†) to be challenging, potentially weakening the effect of conjugation. This is reflected in the high activity of carbonyl C to the nucleophile and decreased selectivity of these methyl substituted probes to GSH. An intense *+ I* effect (electron-donating inductive effect) generated by methoxyl can enhance the electron density on the acrylic ester moiety, passivate the activation on the $\beta$ site of carbonyl, and eliminate the possibility of reaction with other nucleophiles aside from GSH. Although methoxyl could lead to excellent selectivity to GSH, it comes at the expense of the reaction rate and signal intensity. So, in this case, the electron donor group could turn out to be a double-edged sword for the construction and modification of "Michael addition reaction" type probes. In contrast, the strong *− I* effect (electron-withdrawing inductive effect) of nitryl will break the conjugated system, decrease the protective effect of carbonyl C, and lead to an extreme instability towards various nucleophiles, causing probes to lose their selectivity.

## Enhanced and optimized design strategy for GSH specific probes

Based on the above research results, we have proposed an enhanced and optimized strategy for a probe template which uses acrylic ester derivatives to mask fluorescence and capture GSH. As depicted in Fig. 4, carbonyl C was stabilized by a conjugated structure (benzene) at the $\beta$-site. The average electron cloud could protect the carbonyl C from the attack of nucleophile factors. To further upgrade this strategy, the introduction of an electron-donating group into the conjugated system can reinforce the stabilizing effect, compelling the deprotection reaction to proceed only through Michael addition at the $\beta$-site of carbonyl C, which creates enhanced selectivity for GSH. In contrast, the probe template modified by an electron-withdrawing group or inserted methyl at the $\alpha/\beta$-site will break or twist the conjugation effect, leading to a GSH non-selective probe.

## Optical properties

In order to validate our strategy, we synthesized the relevant probes and systematically analyzed their optical properties. Spectroscopic properties of each probe (20 μM) were evaluated with 50 equiv. of various analytes in aqueous solution (DMSO/$H_2O$ = 1/9, 0.1 M PBS, pH = 7.4, $\lambda_{ex}$ = 470 nm) buffer.

For example, take **Fl-H** as a representative probe (Fig. 5a), as expected, **Fl-H** alone was virtually non-fluorescent and showed a dramatic increase in fluorescence at 530 nm when 50 equiv. GSH was added to the system. By contrast, other analytes including potentially interfering thiols, such as Cys, Hcy, and $H_2S$, hardly triggered any fluorescent signal from **Fl-H** (front bars). The addition of competing thiols, along with GSH, indicated that probe **Fl-H** was able to differentiate GSH from other thiols at high concentrations (back bars). This is in accordance with the relatively weak reaction activity of **Fl-H** with GSH that was described in the structure–activity analysis.

To further evaluate the performance of **Fl-H** for the detection of GSH *in vitro*, we investigated the ability of **Fl-H** to sense GSH quantitatively (Fig. 5b). An emission peak at 530 nm gradually increased as increasing concentrations of GSH (0–80 equiv.) were added to the solution with probe **Fl-H**. The linear relationship indicated that **Fl-H** could quantify GSH in the range of 2–50 equiv. of its own concentration (Fig. 5c and d). The optical properties of **Fl-2/3/4OMe** were similar to those of **Fl-H**, and their optical spectra are shown in Fig. S1–S13.†

In order to investigate how different substituent groups on the probes influenced performance, we performed a time response experiment (Fig. 6). **Fl-H** and **Fl-2/3/4OMe** are fairly stable in PBS buffer solution (0.1 M, pH = 7.4) and exhibit good performance for GSH detection. It is obvious that **Fl-H** has a higher intensity than probes with methyl substituents after the fluorescence intensity stabilizes. In fact, their intensities correspond to their substitutional position on the benzene ring

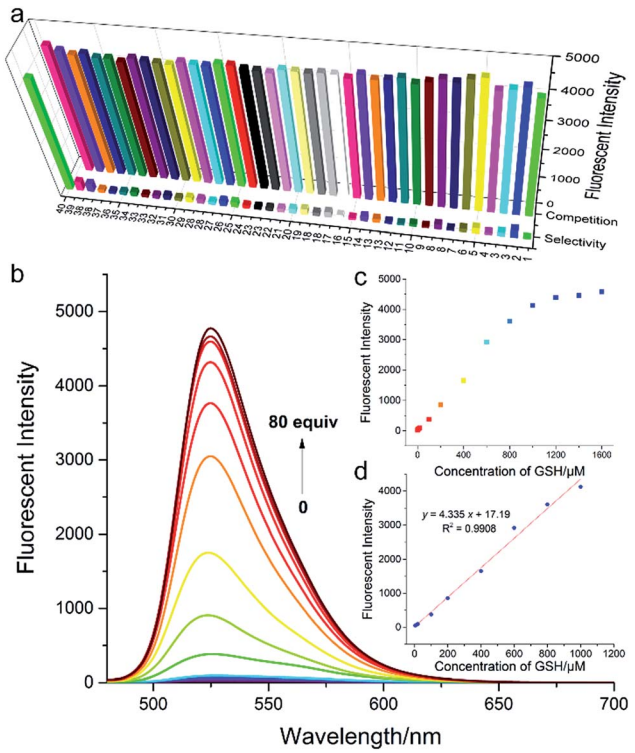


Fig. 5 (a) Front row: fluorescence intensity of **Fl-H** (20 μM) upon the addition of varied analytes (1 mM); back row: fluorescence intensity of **Fl-H** (20 μM) upon the addition of GSH (1000 μM) in the presence of various analytes (2 mM). (1) Blank; (2) $H_2S$; (3) Ala; (4) Arg; (5) Cys; (6) Glu; (7) Hcy; (8) Ile; (9) Leu; (10) Lys; (11) Met; (12) Phe; (13) Pro; (14) Ser; (15) Thr; (16) Trp; (17) Tyr; (18) Val; (19) Sec; (20) ascorbic acid; (21) tocopherol; (22) NO; (23) $N_3^-$; (24) $NO_2^-$; (25) HNO; (26) $ONOO^-$; (27) $O_2^-$; (28) $H_2O_2$; (29) $ClO^-$; (30) $Br^-$; (31) $Cl^-$; (32) $SO_3^{2-}$; (33) $HSO_3^-$; (34) $S_2O_3^{2-}$; (35) $HSO_4^-$; (36) $SO_4^{2-}$; (37) $S_8$; (38) $Na_2S_2$; (39) $Na_2S_4$; (40) GSH; (b) fluorescence spectra of **Fl-H** (20 μM) upon addition of increasing concentrations of GSH (0–80 equiv.) after 2 h. (c) Fluorescence intensity at 530 nm of each concentration of GSH. (d) Linear relationship in the range of 0–50 equiv. GSH. Each spectrum and dataset was acquired in DMSO/$H_2O$ = 1/9, 0.1 M PBS, pH = 7.4, $\lambda_{ex}$ = 470 nm.

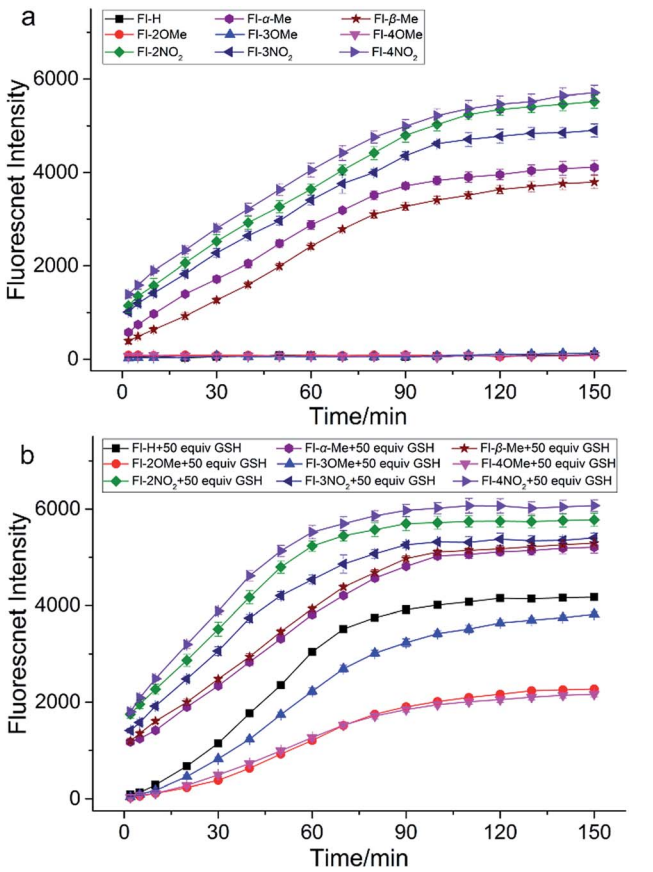


Fig. 6 (a) Fluorescence intensity changes of all probes in 150 min; (b) fluorescence intensity changes of probe + 50 equiv. GSH in 150 min. DMSO/$H_2O$ = 1/9, 0.1 M PBS, pH = 7.4. Data were recorded at 530 nm, $\lambda_{ex}$ = 470 nm.

(**Fl-H** > **Fl-3OMe** > **Fl-2OMe** ≈ **Fl-4OMe**). It takes nearly 90 min for the fluorescence intensity of **Fl-H/3OMe** to stabilize with GSH, and 120 min for **Fl-2/4OMe.** These probes also have remarkable stability for other thiols. These results demonstrated that the electron donor group could slow down the recognition reaction and provide good selectivity for the detection of GSH, as we predicted in the optimized strategy. Furthermore, **Fl-H/2/3/4OMe** could withstand a wide pH range of 6–9, indicating potential applications under physiological conditions. In contrast, **Fl-α/βMe** and **Fl-2/3/4NO$_2$** are unstable and non-selective for GSH in PBS buffer solution, since the Michael addition reaction was inhibited by the steric hindrance of a dense electron cloud making the carbonyl C atom the first attacked site. Furthermore, the positively guided GSH specific probes (**Fl-H/2/3/4OMe**) exhibited good photostability both *in vitro* and *in vivo* (Fig. S18–S25†). All of these reaction kinetics and fluorescence intensities essentially agree with theoretical calculation results.

Additionally, probes dually protected by acrylate derivatives were also synthesized and investigated. The fluorescence masking effects of **Di-Fl-H** and **Di-Fl-2/3/4OMe** were too strong to be activated by any of all these analytes, including GSH. **Di-Fl-α/βMe** and **Di-Fl-2/3/4NO$_2$** were unstable and non-selective in PBS buffer solution with a much faster rate, at close to 30 min than monosubstituted probes.

## Proposed mechanism for GSH probes

To give a more explicit picture of the performance regulation and control strategy, we have proposed a recognition mechanism for our GSH probes in Fig. 7. When **R** = **H** or **2/3/4OMe**, **R′** = **R″** = **H**, the ester bond was stabilized by the leveling effect of a strong conjugated benzene, and GSH was inclined to attack at the enone β-carbon. Then, the generated recognition intermediate **probe-GSH** was hydrolyzed under alkalescence or esterase to produce fluorescein and release a fluorescent signal. Substitution by nitryl or methyl at the displayed position would accelerate esterolysis, leading to the release of the fluorophore in a distinct way.

## Biological imaging

Cytotoxicity experiments demonstrated the minimal cytotoxicity of **Fl-H/2/3/4OMe** toward MCF-7 cells at a concentration over 100 μM (Fig. S26†) by the standard MTT assay, indicating

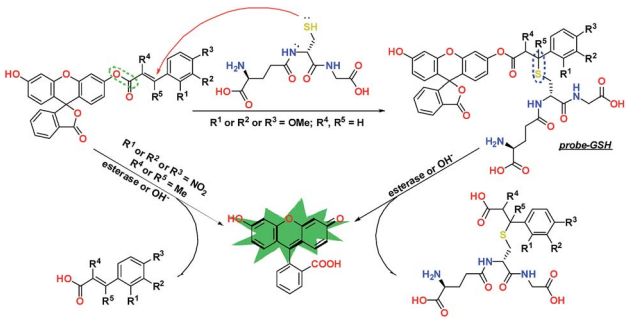


Fig. 7 Proposed mechanism for GSH probes.

excellent biocompatibility. We then examined the potential of these probes to visualize GSH in live MCF-7 cells with confocal fluorescence microscopy. When pure probes (20 μM) were added to the cell system, a strong green fluorescence enhancement appeared under the exposure of 488 nm laser light after 0.5 h (Fig. 8b–d). In order to validate that the detection efficiency was actually from endogenous GSH, cells were treated with 2 mM α-LPA (α-lipoic acid) for 12 h, followed by 20 μM probes for 0.5 h (Fig. 8h–j). The cells showed an obviously stronger green fluorescent signal after being washed with PBS three times. In addition, when 2 mM NEM (*N*-ethylmaleimide) was used to reduce cellular GSH levels for 2 h before the probe was introduced into the cultured system, the fluorescence intensity significantly decreased (Fig. 8e–g). Furthermore, it's easy to discover that the response speed of these probes was much faster than it was *in vitro*. And in order to explore the causes leading to this phenomenon, a time-dependent experiment at 37 °C with esterase and without esterase was carried out (Fig. S14†). The fluorescence intensity of these positively guided probes stabilized in 60 min when 50 equiv. GSH was added into the solution at 37 °C, and the addition of esterase could reduce the reaction time to 40 min. In contrast, at room temperature without the addition of esterase, the reaction time increased to 120 min. These time-dependent experiments strongly illustrate the synergistic effect of physiological environment temperature and esterase could promote the recognition behavior of these probes. These results illustrated that the probes actually detected endogenous GSH in cells, suggesting that these probes could be used to determine the GSH concentration in relevant disease states.

## Conclusions

In conclusion, we have constructed a general template for GSH probes and proposed a practical regulation strategy to improve their recognition performance. With this strategy, we have developed a series of congeneric probes based on protection–deprotection using various acrylic ester derivatives and analyzed their optical performance systematically. Through the combination of theory and practice, we have validated that a conjugative effect-enhanced acrylate moiety has a remarkable selectivity for GSH over other thiols. Electron donor groups can increase the conjugative effect and improve the selectivity, but electron withdrawing groups have the exact opposite effect. Furthermore, the insertion of a methyl group into the $\alpha/\beta$ site of the carbonyl C would interfere with the conjugative effect, leading to a probe that is non-selective for GSH. More importantly, the well-designed probes were excellent for mapping GSH *in vivo*, which demonstrated the applicability of our guiding strategy. Our practical design strategy has profound significance for the recognition performance of GSH probes and great value for improving the performance of reaction-based probes.

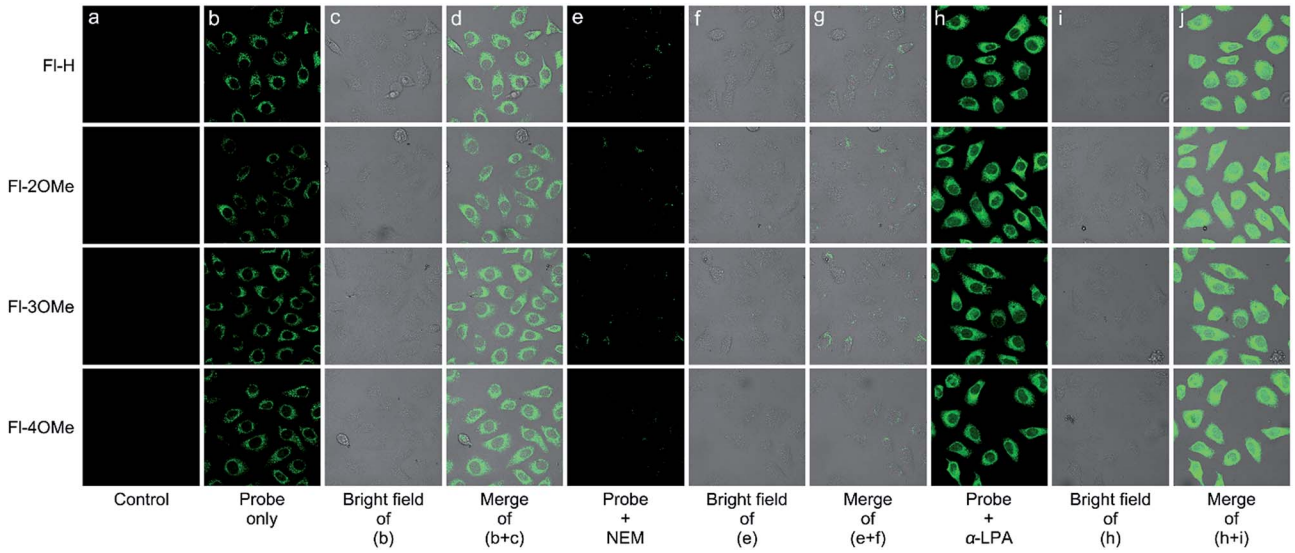


Fig. 8 Confocal laser scanning microscopy images of MCF7 cells treated with probes **Fl-H/2/3/4OMe** (20 μM, 2 h, $\lambda_{ex}$ = 488 nm) in the presence/absence of α-LPA or NEM. (a) Control; (b) cells treated with probes only; (c) bright field of b; (d) merge of b and c; (e) cells treated with 2 mM NEM for 12 h, and then treated with probes **Fl-H/2/3/4OMe**; (f) bright field of e; (g) merge of e and f; (h) cells treated with 2 mM α-LPA for 12 h, and then treated with probes **Fl-H/2/3/4OMe**; (i) bright field of e; (j) merge of h and i.

## Conflicts of interest

The authors declare that they have no competing financial interests.

## Acknowledgements

This work was supported by the National Natural Science Foundation of China (NSFC 21572177 and 21673173), China Postdoctoral Science Foundation (No. 2017M623225), Natural Science Basic Research Plan in Shaanxi Province of China (No. 2016JZ004 and 2018JQ3038), and the Northwest University Science Foundation for Postgraduate Students (No. YZZ17123 and YZZ17124). All the live subject procedures were conducted in accordance with the Experimental Animal Administration regulations issued by the State Committee of Science and Technology of the People's Republic of China and Experiments were approved by the Animal Ethics Committee of Northwest University.

## References

1 T. Ren, Q. Zhang, D. Su, X. Zhang, L. Yuan and X. Zhang, *Chem. Sci.*, 2018, **9**, 5461–5466.
2 L. Yuan, W. Lin, K. Zheng, L. He and W. Huang, *Chem. Soc. Rev.*, 2013, **42**, 622–661.
3 T. Liu, Z. Xu, D. R. Spring and J. Cui, *Org. Lett.*, 2013, **15**, 2310–2313.
4 S. Lim, K. Hong, D. Kim, H. Kwon and H. Kim, *J. Am. Chem. Soc.*, 2014, **136**, 7018–7025.
5 L. He, X. Yang, Y. Liu, X. Kong and W. Lin, *Chem. Commun.*, 2016, **52**, 4029–4032.
6 A. Chen and S. Chatterjee, *Chem. Soc. Rev.*, 2013, **42**, 5425–5438.
7 X. Chen, Y. Zhou, X. Peng and J. Yoon, *Chem. Soc. Rev.*, 2010, **39**, 2120–2135.
8 M. Ye, X. Wang, J. Tang, Z. Guo, Y. Shen, H. Tian and W. Zhu, *Chem. Sci.*, 2016, **7**, 4958–4965.
9 N. Zhao, Q. Gong, R. Zhang, J. Yang, Z. Huang, N. Li and B. Tang, *J. Mater. Chem. C*, 2015, **3**, 8397–8402.
10 Y. Sun, J. Liu, H. Zhang, Y. Huo, X. Lv, Y. Shi and W. Guo, *J. Am. Chem. Soc.*, 2014, **136**, 12520–12523.
11 M. Cao, H. Chen, D. Chen, Z. Xu, S. Liu, X. Chen and J. Yin, *Chem. Commun.*, 2016, **52**, 721–724.
12 D. Wu, A. C. Sedgwick, T. Gunnlaugsson, E. U. Akkaya, J. Yoon and T. D. James, *Chem. Soc. Rev.*, 2017, **46**, 7105–7123.
13 H. Chen, Y. Tang, M. Ren and W. Lin, *Chem. Sci.*, 2016, **7**, 1896–1903.
14 L. He, X. Yang, K. Xu, X. Kong and W. Lin, *Chem. Sci.*, 2017, **8**, 6257–6265.
15 H. Jung, X. Chen, J. Kim and J. Yoon, *Chem. Soc. Rev.*, 2013, **42**, 6019–6031.
16 J. Yin, Y. Kwon, D. Kim, D. Lee, G. Kim, Y. Hu, J. H. Ryu and J. Yoon, *J. Am. Chem. Soc.*, 2014, **136**, 5351–5358.
17 J. Liu, X. Zhang, Z. Cong, Z. Chen, H. Yang and G. Chen, *Nanoscale*, 2013, **5**, 1810–1815.
18 R. Kawagoe, I. Takashima, S. Uchinomiya and A. Ojida, *Chem. Sci.*, 2017, **8**, 1134–1140.
19 P. Shukla, V. S. Khodade, M. Sharath Chandra, P. Chauhan, S. Mishra, S. Siddaramappa, B. E. Pradeep, A. Singh and H. Chakrapani, *Chem. Sci.*, 2017, **8**, 4967–4972.
20 Z. Liu, X. Zhou, Y. Miao, Y. Hu, N. Kwon, X. Wu and J. Yoon, *Angew. Chem., Int. Ed.*, 2017, **56**, 5812–5816.
21 Y. Ahn, J. Lee and Y. Chang, *J. Am. Chem. Soc.*, 2007, **129**, 4510–4511.
22 L. Niu, Y. Guan, Y. Chen, L. Wu, C. Tung and Q. Yang, *J. Am. Chem. Soc.*, 2012, **134**, 18928–18931.
23 Y. Yang, T. Cheng, W. Zhu, Y. Xu and X. Qian, *Org. Lett.*, 2010, **13**, 264–267.
24 S. Lee, J. Li, X. Zhou, J. Yin and J. Yoon, *Coord. Chem. Rev.*, 2018, **366**, 29–68.
25 J. Li, Y. Kwon, K. Chung, C. Lim, D. Lee, Y. Yue, J. Yoon, G. Kim, S. Nam, Y. Chung, H. Kim, C. Yin, J. Ryu and J. Yoon, *Theranostics*, 2018, **8**, 1411–1420.
26 X. Zhang, C. Zheng, S. Guo, J. Li, H. Yang and G. Chen, *Anal. Chem.*, 2014, **86**, 3426–3434.
27 H. Xiang, H. Tham, M. Nguyen, S. Fiona Phua, W. Lim, J. Liu and Y. Zhao, *Chem. Commun.*, 2017, **53**, 5220–5223.
28 F. Wang, L. Zhou, C. Zhao, R. Wang, Q. Fei, S. Luo, Z. Guo, H. Tian and W. Zhu, *Chem. Sci.*, 2015, **6**, 2584–2589.
29 M. Işık, R. Guliyev, S. Kolemen, Y. Altay, B. Senturk, T. Tekinay and E. U. Akkaya, *Org. Lett.*, 2014, **16**, 3260–3263.
30 X. Yang, Q. Huang, Y. Zhong, Z. Li, H. Li, M. Lowry, J. O. Escobedo and R. M. Strongin, *Chem. Sci.*, 2014, **5**, 2177–2183.
31 Y. Yue, F. Huo, P. Ning, Y. Zhang, J. Chao, X. Meng and C. Yin, *J. Am. Chem. Soc.*, 2017, **139**, 3181–3185.
32 J. Guo, S. Yang, C. Guo, Q. Zeng, Z. Qing, Z. Cao, J. S. Li and R. Yang, *Anal. Chem.*, 2018, **90**, 881–887.
33 Y. Qi, Y. Huang, B. Li, F. Zeng and S. Wu, *Anal. Chem.*, 2017, **90**, 1014–1020.
34 D. Qi, L. Zhang, L. Wan, Y. Zhang, Y. Bian and J. Jiang, *Phys. Chem. Chem. Phys.*, 2011, **13**, 13277–13286.
35 D. Qi, L. Zhang, L. Zhao, X. Cai and J. Jiang, *ChemPhysChem*, 2012, **13**, 2046–2050.
36 A. D. Becke, *J. Chem. Phys.*, 1993, **98**, 5648–5652.
37 M. J. Frisch, G. W. Trucks, H. B. Schlegel, G. E. Scuseria, M. A. Robb, J. R. Cheeseman, G. Scalmani, V. Barone, B. Mennucci, G. A. Petersson, H. Nakatsuji, M. Caricato, X. Li, H. P. Hratchian, A. F. Izmaylov, J. Bloino, G. Zheng, J. L. Sonnenberg, M. Hada, M. Ehara, K. Toyota, R. Fukuda, J. Hasegawa, M. Ishida, T. Nakajima, Y. Honda, O. Kitao, H. Nakai, T. Vreven, J. A. Montgomery Jr, J. E. Peralta, F. Ogliaro, M. J. Bearpark, J. Heyd, E. N. Brothers, K. N. Kudin, V. N. Staroverov, R. Kobayashi, J. Normand, K. Raghavachari, A. P. Rendell, J. C. Burant, S. S. Iyengar, J. Tomasi, M. Cossi, N. Rega, N. J. Millam, M. Klene, J. E. Knox, J. B. Cross, V. Bakken, C. Adamo, J. Jaramillo, R. Gomperts, R. E. Stratmann, O. Yazyev, A. J. Austin, R. Cammi, C. Pomelli, J. W. Ochterski, R. L. Martin, K. Morokuma, V. G. Zakrzewski, G. A. Voth, P. Salvador, J. J. Dannenberg, S. Dapprich, A. D. Daniels, Ö. Farkas, J. B. Foresman, J. V. Ortiz, J. Cioslowski and D. J. Fox, *Gaussian 09*, Wallingford, CT, USA, 2009.

 